Journal of Economic Behavior & Organization 99 (2014) 32–52

Contents lists available at ScienceDirect

Journal of Economic Behavior & Organization

journal homepage: www.elsevier.com/locate/jebo

Self-organization of hexagonal agglomeration patterns in new economic geography models

Kiyohiro Ikeda[a,*], Kazuo Murota[b], Takashi Akamatsu[c], Tatsuhito Kono[d], Yuki Takayama[e]

[a] Department of Civil and Environmental Engineering, Tohoku University, 6-6-06 Aoba, Sendai 980-8579, Japan
[b] Department of Mathematical Informatics, University of Tokyo, Tokyo 113-8656, Japan
[c] Graduate School of Information Sciences, Tohoku University, 6-6-06 Aoba, Sendai 980-8579, Japan
[d] Graduate School of Information Sciences, Tohoku University, 6-3-09 Aoba, Sendai 980-8579, Japan
[e] Graduate School of Science and Engineering, Ehime University, 3 Bunkyo-cho, Matsuyama 790-8577, Japan

ARTICLE INFO

Article history:
Received 12 November 2012
Received in revised form 17 August 2013
Accepted 14 December 2013
Available online 2 January 2014

JEL classification:
R12
R13
C65
F12

Keywords:
Bifurcation
Central place theory
Core–periphery models
Group-theoretic bifurcation theory
Hexagons
New economic geography
Self-organization

ABSTRACT

Self-organization of agglomeration patterns for economic models in a two-dimensional economic space is studied from a multi-disciplinary viewpoint of new economic geography, central place theory, and bifurcation theory. Emergence of hexagonal distributions of various sizes in a homogeneous space is predicted theoretically for core–periphery models. The existence of hexagonal distributions as stable equilibria is demonstrated by a comparative static analysis with respect to transport costs for specific core–periphery models. These distributions are the ones envisaged by central place theory and also inferred to emerge by Krugman (1996) for a core–periphery model in two dimensions.

© 2014 Elsevier B.V. All rights reserved.

1. Introduction

The evolution of economic agglomeration in cities is a vital factor of economic growth, and its study is an important topic in economic geography.[1] An accepted scenario of this agglomeration is the self-organization of a few large cities from evenly spread economic activities associated with the progress of transportation technology, trade liberalization, and economic integration.

A question to be answered is, “*Where* and *how* is spatial agglomeration self-organized?” Where agglomeration occurs was first studied in central place theory by Christaller (1933), who envisaged the self-organization of market areas of various sizes in a two-dimensional space. *How* self-organization takes place was elucidated not by Christaller’s study, but by a study

* Corresponding author. Tel.: +81 22 795 7416; fax: +81 22 795 7418.
E-mail address: ikeda@civil.tohoku.ac.jp (K. Ikeda).

[1] See, e.g., Clarke and Wilson (1985) and Munz and Weidlich (1990) for early studies of self-organizing patterns in geography and regional science.

0167-2681/$ – see front matter © 2014 Elsevier B.V. All rights reserved.
http://dx.doi.org/10.1016/j.jebo.2013.12.008

of Krugman (1991). He introduced the Dixit–Stiglitz model (1977) of monopolistic competition into spatial economics, and modeled product market imperfections occurring in conjunction with increasing returns, transportation costs, and factor mobility. Thereafter, this model blossomed into new economic geography, which is acknowledged as an important branch of international, regional, and urban economics. The modeling, however, remained one-dimensional and the problem of *where* agglomeration occurs is yet to be fully answered. The objective of this paper is to answer *where* and *how* economic agglomeration takes place in a two-dimensional space based on a multi-disciplinary viewpoint of new economic geography, central place theory, and bifurcation theory.

In central place theory of economic geography (Appendix A), Christaller (1933) envisaged self-organization of hexagonal market areas of various sizes in an infinite uniform space in two steps: (1) formation of hexagons of a single size for a single industry and (2) that of overlapping hexagons of various sizes for multi-industries. He demonstrated the dominance of such self-organization in determining the distribution of central places in southern Germany, and his study contributed to empirical investigations of several places, such as Snohomish County (Washington), Southwestern Iowa, Southwestern Ontario, the Niagara Peninsula, and so on (Dicken and Lloyd, 1990, pp.39–43). Sanglier and Allen (1989) used a dynamic model based on central place theory and successfully calibrated the model with socio-economic data for Belgium, 1970–84.

Although "it (central place theory) is a powerful idea too good for being left as an obscure theory" (Fujita et al., 1999a), this theory is based only on a normative and geometrical approach and is not derived from market equilibrium conditions. To reinforce this theory not only from a geographical standpoint but also from an economic viewpoint, it is necessary to give it the following two underpinnings: (i) a microeconomic mechanism for the location equilibrium and (ii) a two-dimensional economic space.

An early attempt to provide central place theory with a microeconomic foundation was made by Eaton and Lipsey (1975, 1982), and a hexagonal distribution of mobile production factors (e.g., firms and workers) in two dimensions was shown to exist as an economic equilibrium for spatial competition (Eaton and Lipsey, 1975). This, however, remained as a partial equilibrium approach and did not investigate the stability of the equilibrium.

In new economic geography, analytical results for these models have been acquired mostly using simple geometries of two places[2] and sometimes employing the racetrack economy,[3] namely, an economy in which initially identical places spread uniformly around the circumference of a circle. Most studies have dealt with a single industry, whereas a few have developed a microeconomic mechanism for multi-industries (Fujita et al., 1999a; Tabuchi and Thisse, 2011).[4] Yet these studies dealt only with one-dimensional economies and relied on the numerical simulation.

The racetrack economy, which is one-dimensional, can accommodate several patterns, and Krugman (1996, p. 91) inferred the following based on the study of a racetrack economy:

> I have demonstrated the emergence of a regular lattice only for a one-dimensional economy, but I have no doubt that a better mathematician could show that a system of hexagonal market areas will emerge in two dimensions.

The limitation of the one-dimensional economy and the need to extend core–periphery models into two dimensions have come to be acknowledged, as cited by Neary (2001, p. 551): "Perhaps it will prove possible to extend the Dixit-Stiglitz approach to a two-dimensional plain." Stelder (2005) conducted a simulation of agglomeration for cities in Europe using a grid of points. Barker (2012) extended the racetrack geometry to two dimensions, conducted a simulation, and compared it with real cities. Although such naïve simulations can yield some information on agglomeration patterns, it is not possible to overcome several difficulties encountered in a two-dimensional economy, such as a plethora of multiple stable equilibria, and theoretical classification and interpretation of these equilibria (Section 4). A firm theoretical basis to classify these equilibria and a systematic methodology to set forth predominant ones must be established to derive implications for policy proposals.

The unification of central place theory and microeconomic mechanisms, which was first attempted by Eaton and Lipsey (1975, 1982), seems to be in sight. Such unification is important in extending the horizon of new economic geography via cross-fertilization with central place theory. As for the aforementioned two underpinnings for central place theory, the first underpinning of a micro economic mechanism seems to have been satisfactorily constructed in new economic geography, whereas the second underpinning of a two-dimensional economic space remains to be constructed.

A proper choice of a spatial platform is an important issue, and there are several candidates (cf., Golubitsky and Stewart, 2002):

- A continuous two-dimensional space without any discretization is an ideal spatial platform. Yet a continuous version of a core–periphery model needs to be developed, and mathematical analysis of this space with large symmetry would become very complicated.

[2] There is a criticism that economic agglomerations, in reality, would emerge at more than two locations, as was stated by Behrens and Thisse (2007) and was empirically evidenced by Bosker et al. (2010).

[3] Agglomeration patterns of the racetrack economy were observed by Krugman (1993), Fujita et al. (1999b), Picard and Tabuchi (2010), Ikeda et al. (2012a), and Akamatsu et al. (2012).

[4] A one-dimensional continuous segment, termed the long narrow economy, was used by Fujita et al. (1999a), combining a core–periphery model for multiple industries with an urban spatial economy. By comparative static analysis with respect to population size, they demonstrated the emergence of an urban hierarchy. Tabuchi and Thisse (2011) studied the racetrack economy for the multi-industry model to produce Christaller-like spatial patterns.

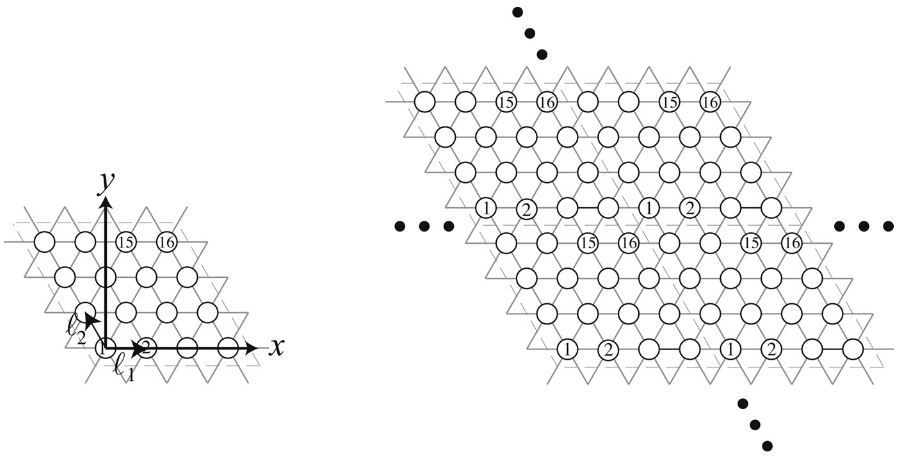

(a) 4 × 4 regular triangular lattice

(b) Spatially repeated 4 × 4 regular triangular lattices

Fig. 1. A system of places on a 4 × 4 regular triangular lattice with periodic boundaries. (a) 4 × 4 regular triangular lattice and (b) spatially repeated 4 × 4 regular triangular lattices.

- A square lattice can engender square, rectangular, and deformed triangular patterns, which are incompatible with hexagonal patterns of our interest.
- A regular triangular lattice[5] can engender triangular, rectangular, and hexagonal patterns.

For this reason, a regular triangular lattice is employed as a two-dimensional economic space in the present study. A *finite* regular triangular lattice consisting of a tightly packed set of regular triangles with periodic boundaries[6] is considered (Fig. 1). The proposal of such a pertinent spatial platform engendering hexagonal distributions is one of the contributions of this paper, whereas other patterns, such as square and rectangular ones, should be investigated in the future.

As an essential theoretical contribution of this paper, the existence of bifurcations that can engender Christaller's hexagonal distributions is proved for core–periphery models with a single industry[7] on a regular triangular lattice.[8] This is in a sharp contrast to the search for bifurcating patterns of the racetrack economy (Ikeda et al., 2012a; Akamatsu et al., 2012), which failed to arrive at hexagonal patterns despite the use of a similar theoretical approach. Bifurcation properties, such as the existence and classification of hexagonal bifurcating patterns, are herein presented. With the aid of these bifurcation properties, stable equilibria are successfully found by comparative static analysis with respect to transportation costs for two specific core–periphery models. The change of stable equilibria associated with a decrease of the transportation cost is investigated in view of a trade-off between scale economies and transportation costs. The abrupt change of stable hexagonal distributions with respect to the parameters is highlighted as a major finding of this paper.

As an important economic implication of this paper, the spatial period of regularly arrayed hexagons for Christaller's distributions is advanced as an important index for the size of the market area. Agglomeration is shown to lead to a system with a larger spatial period when transportation cost decreases. The spatial period advanced herein thus offers a theoretical foundation for *agglomeration shadow*.[9] This paper is organized as follows. The governing equation for two specific core–periphery models is presented in Section 2. The existence of bifurcating hexagonal distributions for a two-dimensional economy is theoretically predicted in Section 3. Computational bifurcation analysis is conducted in Section 4 to find stable equilibria for Christaller's hexagonal distributions and to examine the economic interpretation of these distributions. Technical details are given in Appendices.

[5] In nonlinear mathematics, hexagonal distributions have been shown to exist on this lattice, which is often called the hexagonal lattice, for several physical problems (Golubitsky and Stewart, 2002). In contrast, in central place theory, the infinite regular triangular lattice is suggested for use based on geometrical discussion (Lösch, 1940; 1954).

[6] Since it is difficult in the framework of core–periphery models to deal with an infinite number of places on the infinite regular triangular lattice analytically or numerically, a *finite* regular triangular lattice with periodic boundaries is used to express uniformity by avoiding heterogeneity due to the boundaries and to express infiniteness by spatially repeating the finite lattice periodically to cover the infinite two-dimensional domain.

[7] A simple modeling of a single industry is considered herein, as the formation of hexagonal patterns has yet to be accomplished even for this simple modeling.

[8] For example, in the convective motion of fluid in the Bénard problem, regularly arrayed hexagons are self-organized (e.g., Koschmieder, 1974). The mechanism of this self-organization can be successfully explained by group-theoretic bifurcation analysis of the bifurcating solutions in a regular triangular lattice (Golubitsky et al., 1988; Golubitsky and Stewart, 2002; Ikeda et al., 2012b).

[9] Arthur (1990) stated: "Locations with large numbers of firms therefore cast an 'agglomeration shadow' in which little or no settlement takes place. This causes separation of the industry." See also Fujita et al. (1999b), Ioannides and Overman (2004), and Fujita and Mori (2005).

2. Core–periphery models

As typical examples of core–periphery models with a single industry, let us consider the following two models, which are endowed with analytical tractability.

(a) The FO model (Forslid and Ottaviano, 2003) that replaces the production function of Krugman with that of Flam and Helpman (1987).
(b) The Pf model (Pflüger, 2004) that replaces, in addition to the production function, the utility function of Krugman with that of the international trade model of Martin and Rogers (1995).

2.1. Basic assumptions

The economy of these models is composed of K places (labeled $i = 1, \ldots, K$), two factors of production (skilled and unskilled labor), and two sectors (manufacturing, M, and agriculture, A). Both H skilled and L unskilled workers consume two final goods: manufacturing sector goods and agricultural sector goods. Workers supply one unit of each type of labor inelastically. Skilled workers are mobile among places, and the number of skilled workers in place i is denoted by h_i ($\sum_{i=1}^{K} h_i = H$). Unskilled workers are immobile and equally distributed across all places with unit density (i.e., $L = 1 \times K$). Hence the population in place i is equal to $h_i + 1$.

The transportation costs for M-sector goods are assumed to take the iceberg form. That is, for each unit of M-sector goods transported from place i to place $j(\neq i)$, only a fraction $1/\phi_{ij} < 1$ arrives. More concretely, the transport cost ϕ_{ij} between places i and j is defined as $\phi_{ij} = \exp(\tau D_{ij})$, where τ is the transport parameter and D_{ij} represents the shortest transportation distance between places i and j. (We define $\phi_{ii} = 1$.)

Core–periphery models follow two stages of equilibria: (i) market (short-run) equilibrium that is defined as the economic state in which workers are assumed to be immobile among places, and (ii) spatial (long-run) equilibrium of the economic state for mobile workers. The second stage, which is used in the derivation of the general form of the governing equation, is dealt with in Section 2.2, while the first stage is presented in Appendix B.2.

2.2. General form of spatial equilibrium conditions

Although diverse core–periphery models have been developed on the basis of an ensemble of economic principles and assumptions, it is possible to present a general form of spatial equilibrium as explained below.

The population h_i of skilled workers at the ith place is chosen as an independent variable, and the vector $\boldsymbol{h} = (h_1, \ldots, h_K)^\top$ is defined. As is customary in comparative static analysis, the transport parameter, say τ, is chosen as the main parameter.

In the description of the spatial equilibrium of core–periphery models, the adjustment dynamics is considered

$$\frac{d\boldsymbol{h}(t)}{dt} = \boldsymbol{F}(\boldsymbol{h}(t), \tau) \tag{1}$$

with some appropriate function $\boldsymbol{F}(\boldsymbol{h}, \tau)$. A stationary point of this adjustment dynamics (1) is defined as $\boldsymbol{h} = \boldsymbol{h}(\tau)$ that satisfies the spatial equilibrium condition:

$$\boldsymbol{F}(\boldsymbol{h}, \tau) = \boldsymbol{0}. \tag{2}$$

The stability of a solution $\boldsymbol{h}$ to (2) can be defined in relation to the associated dynamical system (1), and the solution is termed linearly stable if every eigenvalue of the Jacobian matrix $J(\boldsymbol{h}, \tau) = \partial \boldsymbol{F}/\partial \boldsymbol{h}$ has a negative real part, and linearly unstable if at least one eigenvalue has a positive real part.

As a specific functional form of $\boldsymbol{F}(\boldsymbol{h}, \tau)$, we employ

$$\boldsymbol{F}(\boldsymbol{h}, \tau) = H\boldsymbol{P}(\boldsymbol{v}(\boldsymbol{h}, \tau)) - \boldsymbol{h}, \tag{3}$$

where $H = \sum_{i=1}^{K} h_i$ is the total sum of the mobile population and $\boldsymbol{P}(\boldsymbol{v}) = (P_1, \ldots, P_K)^\top$ is the choice function vector, which is a function of the indirect utility function vector $\boldsymbol{v} = (v_1, \ldots, v_K)^\top$.

We employ the logit choice function $P_i = P_i(\boldsymbol{v})$ given by

$$P_i(\boldsymbol{v}) = \frac{\exp[\theta v_i]}{\sum_{j=1}^{K} \exp[\theta v_j]}, \tag{4}$$

where $\theta \in (0, \infty)$ is a positive parameter.[10] The adjustment process described by (1) and (3) with (4) is the logit dynamics.[11] In the limit of a $\theta \longrightarrow \infty$, the spatial equilibrium condition (2) with this logit choice function reduces to the following well-known complementarity condition:

$$\begin{cases} (v_i(\boldsymbol{h}, \tau) - \bar{v})h_i = 0, \quad v_i(\boldsymbol{h}, \tau) - \bar{v} \leq 0, \quad h_i \geq 0, \quad i = 1, \ldots, K, \\ \displaystyle\sum_{i=1}^{K} h_i - H = 0. \end{cases}$$

Here, $\bar{v}$ is the equilibrium utility.

The difference of models can be ascribed to the difference of the form of the function $v_i(\boldsymbol{h}, \tau)$. For example, a concrete form this function for specific models is given in (A.11) in Appendix B.

3. Bifurcation of a regular triangular lattice: theoretical analysis

As an essential theoretical contribution of this paper, Christaller's hexagonal distributions are proved to exist as bifurcating solutions in an economy on a regular triangular lattice.[12] The regular triangular lattice and Christaller's hexagonal distributions on this lattice are introduced in Section 3.1, and several important bifurcation properties are advanced in Proposition 1 in Section 3.2.

3.1. Christaller's hexagonal distributions in two-dimensional economic space

A regular triangular lattice with periodic boundaries is introduced as a spatial platform for the core–periphery models, and Christaller's hexagonal distributions on this lattice are presented.

3.1.1. Regular triangular lattice and Christaller's hexagonal distributions

As a two-dimensional economic space, let us consider a finite regular triangular lattice with periodic boundaries comprising uniformly spread $n \times n$ places (Fig. 1(a)). Goods are transported along the homogeneous transportation link of this lattice connecting neighboring places by straight roads of the same length. By virtue of these periodic boundaries, the finite lattice can be repeated spatially to cover an infinite two-dimensional space, and every place is linked to six hexagonal neighboring places (Fig. 1(b)). This lattice can be considered as a discretized counterpart of the isotropic plain in central place theory.[13]

Christaller's hexagonal distributions, termed $k = 3$, 4, and 7 systems, on the regular triangular lattice are shown in Fig. 2(b)–(d). In central place theory (Appendix A), the k value has a geometrical implication in that it is proportional to the size (area) of the hexagonal distribution and its square root $\sqrt{k}$ is proportional to the shortest Euclidian distance L between the first-level centers, i.e., the spatial period of these centers. Geometrically, it is shown that the spatial period L takes some specific values (Appendix C.1 and Lösch, 1940), such as

$$\frac{L}{d} = \sqrt{k}, \quad k = 1, 3, 4, 7, 9, 12, 13, 16, 19, 21, 25, \ldots, \tag{5}$$

where d is the distance between two neighboring places. The smallest value $k = 1$ corresponds to the flat earth equilibrium (uniform distribution). The next three smallest values of $k = 3$, 4, and 7 are associated with Christaller's $k = 3$, 4, and 7 systems, respectively.

Remark 1. Let us consider Christaller's $k = 3$ system on the 3×3 regular triangular lattice shown in Fig. 3(a). This system has the distribution of population $\boldsymbol{h} = (a, b, b\,; b, b, a\,; b, a, b)^\top$ in (A.15) in Appendix C.1, where a is the population for the first-level centers and b is that for the second-level centers. This distribution is repeated spatially to arrive at the distribution for the $k = 3$ system in Fig. 3(b), which covers an infinite space. The hexagonal window in Fig. 2(b) is cut out from this distribution. The $k = 4$ system and $k = 7$ system can be treated similarly. □

3.1.2. Euclidian distance and transportation distance

Recall that the distance D_{ij} between places i and j for the transportation of goods must be defined in the core–periphery models (Section 2.1). For the regular triangular lattice, this distance is measured along the shortest link of the lattice. On the other hand, the spatial period L between neighboring first-level centers is measured by the Euclidian distance. These two kinds of distances for these centers are the same for the $k = 4$ system, but are different for the $k = 3$ system and the $k = 7$

[10] In the spatial equilibrium, the skilled workers are assumed to be heterogeneous in their preferences for location choice; see, e.g., Tabuchi and Thisse (2002), Murata (2003), and Akamatsu et al. (2012). The parameter θ in (4) denotes the inverse of variance of the idiosyncratic taste, which is assumed to follow the Gumbel distribution that is identical across places (e.g., McFadden, 1974; Anderson et al., 1992).

[11] The logit dynamics has been studied in evolutionary game theory (e.g., Fudenberg and Levine, 1998; Hofbauer and Sandholm, 2007; Sandholm, 2010).

[12] This proof is a generalization of a mathematical study (Ikeda et al., 2012b) conducted on a specific core–periphery model, the FO model (Appendix B).

[13] The lattice satisfies Assumptions (i)–(iv) in Appendix A in a discretized sense.

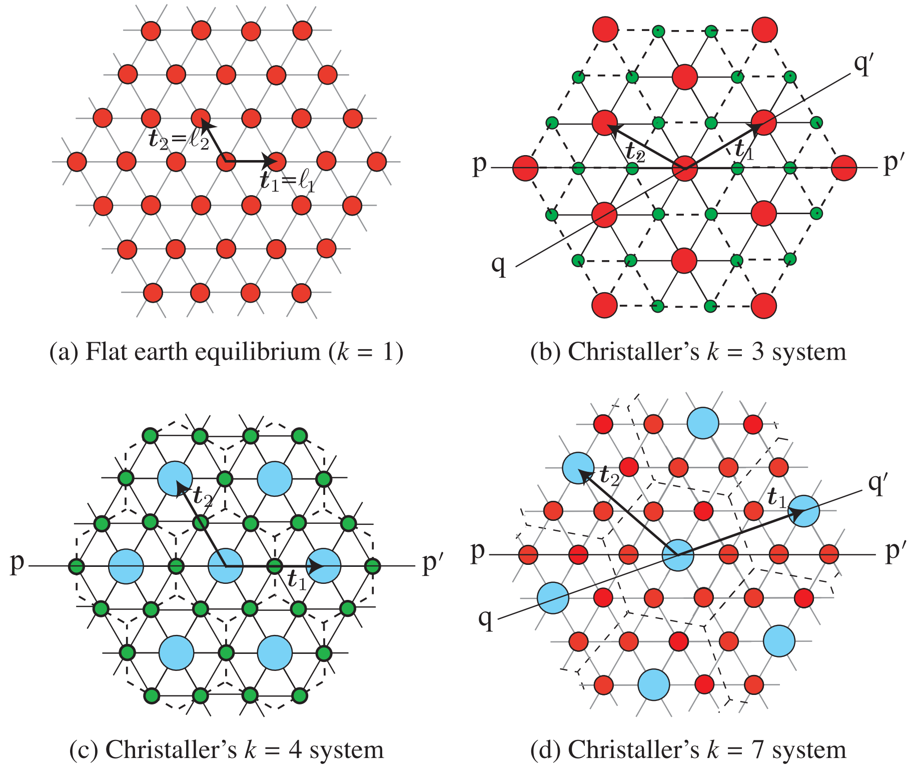

Fig. 2. Hexagonal distributions on the regular triangular lattice (the larger circles represent the first-level centers and the smaller ones the second-level centers). (a) Flat earth equilibrium (k = 1), (b) Christaller's k = 3 system, (c) Christaller's k = 4 system and (d) Christaller's k = 7 system.

system, as explained below. In this connection, it is convenient to classify the normalized spatial periods L/d into two kinds: normalized spatial periods of integer numbers and those of non-integer numbers.

For normalized spatial periods of integer numbers:

$$\frac{L}{d} = \sqrt{k} = 1, 2, 3, 4, 5, \ldots, \quad k = 1, 4, 9, 16, 25, \ldots, \tag{6}$$

two neighboring first-level centers are connected by a straight road along the regular triangular lattice; therefore, the transportation distance and the Euclidian distance between neighboring first-level centers are the same. For example, for the k = 4 system (Fig. 2(c)), the straight line pp′ along the hexagonal grid comprises alternation of a first-level center and a second-level center, and the transportation between neighboring first-level centers is conducted efficiently through a straight road with the distance $D_{ij}/d = L/d = 2$. Such efficient transportation is termed the *traffic principle* in central place theory (Appendix A).

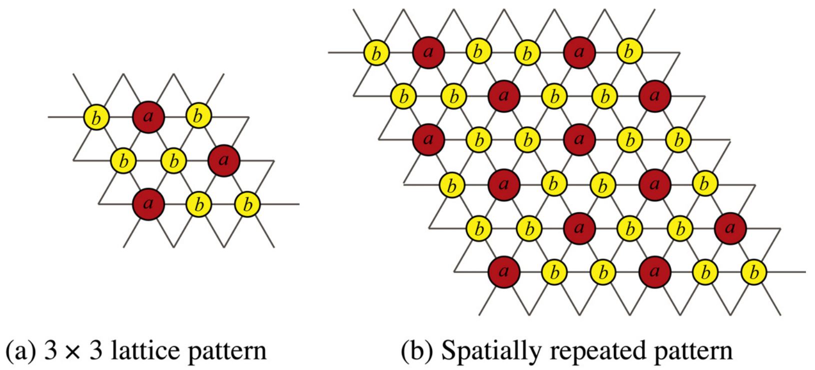

Fig. 3. The pattern for k = 3 system obtained by repeating the pattern for 3 × 3 places (a > b). (a) 3 × 3 lattice pattern (b) Spatially repeated pattern

Table 1
Existence of $k = 3, 4, 7$ systems for several values of n (○ denotes existence and × denotes non-existence).

n	$k = 3$ system	$k = 4$ system	$k = 7$ system
2	×	○	×
3	○	×	×
4	×	○	×
5	×	×	×
6	○	○	×
⋮	⋮	⋮	⋮
41	×	×	×
42	○	○	○
43	×	×	×

For normalized spatial periods of non-integer numbers:

$$\frac{L}{d} = \sqrt{3}, \sqrt{7}, \sqrt{12}, \sqrt{13}, \sqrt{19}, \sqrt{21}, \ldots, \quad k = 3, 7, 12, 13, 19, 21, \ldots, \tag{7}$$

two neighboring first-level centers are not connected by a straight road but by zigzag ones along the regular triangular lattice; therefore, those two kinds of distances are not the same. For example, for the $k = 3$ system (Fig. 2(b)), the spatial period of $L/d = \sqrt{3}$ is measured along the straight line qq′ that does not trace the hexagonal grid, and is shorter than the transportation distance $D_{ij}/d = 2$ between those first-level centers. The traffic principle is not applicable in this case. A similar discussion holds for the $k = 7$ system in Fig. 2(d).

3.2. Bifurcations for Christaller's hexagonal distributions

In proving the existence of bifurcations engendering Christaller's hexagonal distributions for general core–periphery models (Section 2.2), the following fact in Lemma 1 plays an important role.

Lemma 1. *A symmetry condition, termed equivariance*

$$T(g)\boldsymbol{F}(\boldsymbol{h}, \tau) = \boldsymbol{F}(T(g)\boldsymbol{h}, \tau), \quad g \in G, \tag{8}$$

holds for the spatial equilibrium condition (2) of core–periphery models on the regular triangular lattice. Here, G denotes the group in (A.17) that expresses the symmetry of the regular triangular lattice and T(g) is the permutation matrix defined by (A.21).

Proof. See Appendix C.3.2.

Lemma 1 enables application of the analytical results for bifurcating hexagonal patterns on the regular triangular lattice to general core–periphery models presented in Section 2.2. These analytical results are summarized in the proposition below (see Appendix C for the outline of the derivation of these results).

Proposition 1. *Bifurcations from the flat earth equilibria of core–periphery models on the regular triangular lattice have the following properties:*

- *Property 1 (flat earth equilibria): Flat earth equilibria are preserved until bifurcation when the transport parameter τ is changed.*
- *Property 2 (existence): Bifurcating equilibria associated with Christaller's $k = 3$, 4, and 7 systems exist if and only if the size n of the lattice is equal, respectively, to*

$$n = \begin{cases} 3m, & k = 3\ \textit{system}, \\ 2m, & k = 4\ \textit{system}, \\ 7m, & k = 7\ \textit{system} \end{cases} \tag{9}$$

  $(m = 1, 2, \ldots)$.
- *Property 3 (bifurcating patterns): Each of the bifurcating paths for Christaller's $k = 3$, 4, 7 systems has a unique symmetry and this symmetry is preserved until further bifurcation takes place.*

The use of these properties in Proposition 1 in the computational bifurcation analysis (Section 4) to obtain Christaller's $k = 3$, 4, and 7 systems is explained below.

Property 1 indicates that it is necessary to investigate the occurrence of bifurcation on the flat earth equilibria, e.g., by eigenanalysis of the Jacobian matrix J of the spatial equilibrium condition (2).

Property 3 indicates the existence of a continuous solution curve of each system with a particular symmetry. (A more detailed account of this symmetry can be found in Appendix C.2).

Eq. (9) in Property 2 gives a pertinent choice of size n of the regular triangular lattice. Table 1 gives a complete list of hexagons for the $k = 3$, 4, and 7 systems existing for several values of n. If we would like to observe each of these systems, small lattice sizes of $n = 3$, 2, and 7, respectively, are sufficient. Yet, as demonstrated in Section 4, it is of great economic interest to investigate the relative relations of the stable equilibria of these three systems on the same lattice. For such investigation, a large lattice size of $n = 42$ must be employed (Corollary 1 below). A larger lattice size of $n = 43$, however, would not produce any of those hexagons. Thus, a naïve choice of lattice size must be avoided. This indicates the importance of the choice of a pertinent lattice size n, and, in turn, the importance of the theoretical analysis presented as Property 2 above.

Corollary 1. *The lattice of size n admits all of Christaller's* $k = 3$, 4, *and* 7 *systems as bifurcated equilibria if and only if n is a multiple of 42, i.e.,* $n = 42m$ $(m = 1, 2, \ldots)$.

Proof. This follows from (9) and the fact that the least common multiple of 2, 3, and 7 is 42.

4. Bifurcation of the regular triangular lattice: computational analysis

In Section 3, the hexagonal distributions for Christaller's $k = 3$, 4, and 7 systems are theoretically predicted to exist as bifurcating equilibria in general core–periphery models on the regular triangular lattice. In this section, the actual existence of hexagonal distributions is ensured by computational analysis of the two specific core–periphery models, the FO model and the Pf model (Section 2), on the regular triangular lattice. A possible course of agglomeration of stable equilibria is presented.

Comparative static analysis with respect to transportation costs is conducted to obtain bifurcating hexagonal distributions in Section 4.1. The dependence of stability on transportation cost is studied in Section 4.2. Robustness of the qualitative behavior against parameter values is confirmed computationally in Section 4.3.

4.1. Bifurcating equilibria for hexagonal distributions

A 42×42 regular triangular lattice is used so as to ensure the co-existence of Christaller's $k = 3$, 4, and 7 systems and, in turn, to investigate the transition of stable equilibria for these systems (Property 2 in Proposition 1 and Corollary 1 in Section 3.2).

The FO model and the Pf model have several parameters (Appendix B.1) that influence bifurcation phenomena. The following set of parameter values that can engender hexagonal distributions for Christaller's three systems is used. The total number H of skilled workers is chosen to be $H = 42$. The constant μ expressing the expenditure share of manufactured goods is $\mu = 0.4$. The constant elasticity σ of substitution between any two varieties is $\sigma = 5.0$. The inverse θ of variance of the idiosyncratic taste in (4) is $\theta = 1000$. The fixed input requirement α is $\alpha = 1.0$. The length d of the link connecting neighboring places is $d = 1/n = 1/42$ (Section 3.1). These parameter values satisfy the so-called no-black-hole condition (Fujita et al., 1999b): $(\sigma - 1)/\sigma = 0.8 > \mu = 0.4$. Robustness analysis for some parameter values is given in Section 4.3.

Fig. 4 shows the curves of the maximum population $h_{\max}$ plotted against the transport parameter τ obtained for the FO model and the Pf model by comparative static analysis, where $h_{\max} = \max(h_1, \ldots, h_K)$ $(K = n^2 = 42 \times 42)$. The flat earth equilibria corresponding to the horizontal line OO′ at $h_{\max} = H/n^2 = 1/42 \approx 0.024$ are stable during OA shown by the solid line (Property 1 in Proposition 1). Among a number of bifurcation points on these equilibria OO′, we specifically examine the three bifurcation points A, B and C engendering Christaller's $k = 3$, 4, and 7 systems, respectively.[14] Secondary and tertiary bifurcations from these three systems have produced $k = 9$, 12, 21, 28, and 36 systems. By virtue of the size n of the lattice being chosen as 42, equilibria with the five shortest spatial periods $L/d = \sqrt{k}$ $(k = 3, 4, 7, 9, 12)$ in (5) are successfully found. The shapes of the bifurcated curves for the FO model and the Pf model are similar, possibly due to the similar microeconomic mechanisms of agglomeration and dispersion of these models.

The population distributions on the bifurcated curves for $k = 3$, 4, and 7 systems for the FO model are shown in hexagonal windows of Fig. 4(a) (the hexagonal distributions for the Pf model are almost identical). The area of a circle indicates the size of the population at the associated place. The first-level centers are evenly scattered and are equidistant from each other, and each first-level center is surrounded by six regular-hexagonal second-level centers. It is possible to define the market areas of first-level centers. These patterns are exactly the same as those in central place theory in Fig. 2 that were envisaged based on normative and geometrical considerations. The emergence of the tilted hexagonal distribution for the $k = 7$ system (curve CHI) that is directed in a different direction than the lattice is the most phenomenal finding of this paper.

4.2. Dependence of stability of equilibria on transportation cost

Stable equilibria, shown by the solid curves in Fig. 4, are of most economic interest, and are discussed in detail.

4.2.1. Change of stable hexagonal distributions

All bifurcating equilibria are unstable just after bifurcation (e.g., curve AD), regain stability near flat parts of the curves (e.g., point D), and become unstable at some bifurcation points on these flat parts (e.g., point E), except for the $k = 4$ system in the Pf model that is unstable throughout. Accordingly, stable equilibria for each system have an associated range of transport

[14] As expounded in Appendix C, these bifurcation points can be classified by their multiplicity M, which is the dimension of the kernel space of the Jacobian matrix J of the spatial equilibrium condition (2). The three bifurcation points A, B, and C, respectively, with $M = 2$, 3, and 12 can be chosen as the ones which produce Christaller's $k = 3$, 4, and 7 systems.

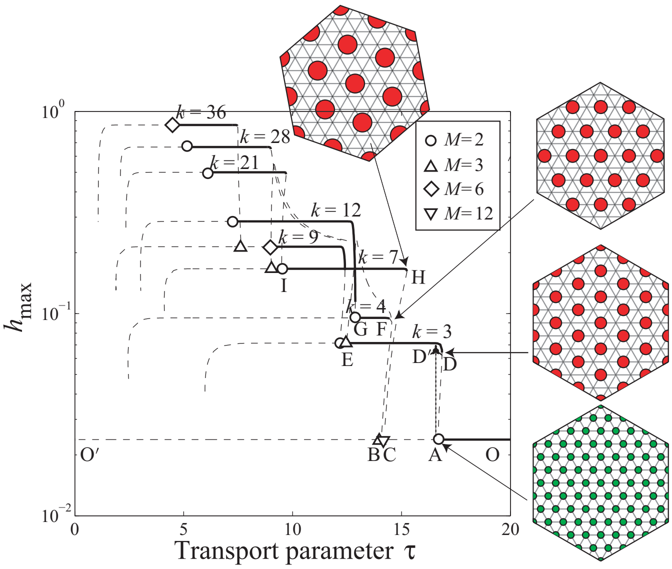

(a) FO model

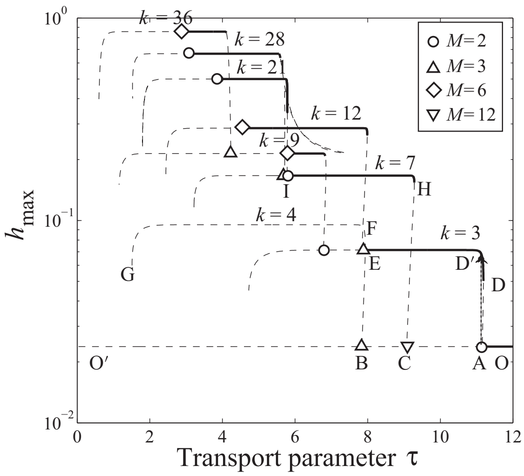

(b) Pf model

Fig. 4. Solution curves (the maximum population h_{max} versus the transport parameter τ curves) for the 42×42 regular triangular lattice computed for the FO model and the Pf model (solid curve: stable; dashed curve: unstable; M is the multiplicity of the bifurcation point (footnote 14); dotted arrow: dynamical shift). (a) FO model (b) Pf model.

parameter τ. For example, the $k=3$ system has the stable range of $\tau_E < \tau < \tau_D$. This range tends to shift toward smaller τ for a larger k, showing a trade-off between transport cost and the size of a system. Relatively wide ranges of stable equilibria are observed for $k=3$, 7, and 12 systems. In contrast, relatively short ranges are observed for $k=4$, 9 and 36 systems.

Since the stability properties of equilibria are similar in both models, we hereafter consider only the Pf model. When the transport parameter τ decreases from a very large value, the change of stable equilibria of several distinct stages can be observed in both models.

- Predominance of the flat earth equilibria ($\tau > \tau_D$): The flat earth equilibria are the only stable ones, and agglomeration is yet to take place.
- Dynamical shift[15] to the $k=3$ system ($\tau_A < \tau < \tau_D$): The flat earth equilibria cease to be stable and the equilibria for the $k=3$ system become stable. A dynamical shift from A to D′ is inevitable to engender agglomeration.

[15] When a stable solution curve becomes unstable at a critical point where a stable bifurcated curve does not exist, the stable curve often shifts dynamically to another stable one. This is called *dynamical shift*.

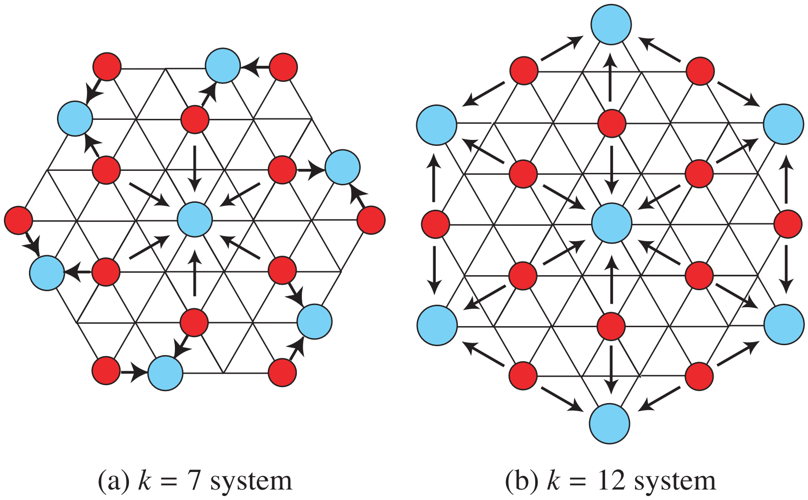

Fig. 5. Conceivable migration of population in the shift from the $k = 3$ system to (a) the $k = 7$ system and to (b) the $k = 12$ system (The size of an arrow indicates the amount of movement; the small circle is the first-level center for the $k = 3$ system and the large one for the $k = 7$ or 12 system.). (a) $k = 7$ system (b) $k = 12$ system.

- Predominance of the $k = 3$ system ($\tau_H < \tau < \tau_A$): The equilibria for the $k = 3$ system are the only stable ones.
- Coexistence of the $k = 3$ system and $k = 7$ system ($\tau_E < \tau < \tau_H$): Only the $k = 3$ system and the $k = 7$ system have stable equilibria, and the equilibria for the $k = 3$ system can dynamically shift to those for the $k = 7$ system under some disturbances.
- Thereafter, $k = 12$, 9, 21, 28, and 36 systems become stable in this order.

In an early stage of agglomeration with high transportation cost, the $k = 3$ system serves as the most important agglomeration pattern that takes place first and remains predominant until the emergence of the stable $k = 7$ system. The next important one is the $k = 7$ system that coexists with the $k = 3$ system as stable equilibria.

A possible early course of change of stable equilibria in association with the decrease of the transport parameter τ is

$$\begin{array}{lllll} k = 1 \text{ system} & \Longrightarrow & k = 3 \text{ system} & \Longrightarrow & k = 7 \text{ system} \\ & & & \searrow & k = 12 \text{ system} \end{array}$$

where $\Rightarrow$ and $\searrow$ denote occurrences of dynamical shifts. The migration of population that is expected to take place in the shift from the $k = 3$ system to the $k = 7$ system is illustrated in Fig. 5(a) and to the $k = 12$ system in (b). The population of the first-level centers of the $k = 3$ system (small circles) migrates to those of the $k = 7$ or 12 system (large circles). Such information on the migration would give us important economic implications for policy proposals, such as the determination of the location for public investment.

Intuitively, the size of the market area (see Fig. 6) for firms is determined by a trade-off between transportation costs and scale economies. Namely, firms at a place with a small market area enjoy a large merit of the reduction of transportation costs at the expense of small scale economies. In contrast, firms at a place with a large market area enjoy a large merit of scale economies at the expense of large transportation cost. When the transportation cost is large, the merit of the reduction of transportation costs is more important, and the $k = 3$ system with the smallest market area becomes more advantageous. When the transportation cost is small, the merit of scale economies is more important, and the $k = 7$ system with a larger market area becomes more advantageous. Such a trade-off prevails for systems with large values of $k = 12$, 21, 28, and 36.

4.2.2. Analogy between two-dimensional economy and two-place economy

It is noteworthy that the equilibria OADE in Fig. 4 associated with the first bifurcation comprise three stages:

- Stable pre-bifurcation stage with the (uniform) population distribution on the flat solution curve OA, which loses stability at the bifurcation point A.
- Unstable bifurcating stage with quickly changing population distribution on the rapidly ascending solution curve AD.
- Stable post-bifurcation stage with almost constant population distribution on the bifurcating curve DE, which loses stability at another bifurcation point E.

Three such stages are also observed for other bifurcating equilibria in Fig. 4, and there are several common features: The population distribution in stable equilibria tends to be preserved, whereas bifurcation is the trigger for a loss of stability leading to the stage of unstable and rapid population change.

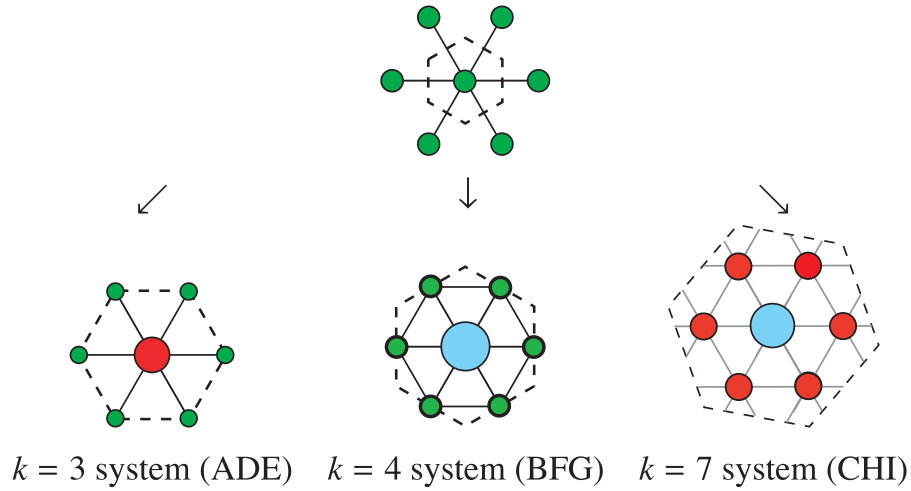

Fig. 6. Market areas for $k=3, 4, 7$ systems (indicated by the dashed lines). $k=3$ system (ADE). $k=4$ system (BFG). $k=7$ system (CHI).

Let us now shift attention to a two-place economy consisting of Place 1 and Place 2 (Fujita et al., 1999b). Figure 7 shows the population versus transport cost curves of this economy of Krugman model (1991) obtained numerically. The aforementioned three stages are observable also in this economy as follows:

- Stable uniform equilibria with a constant population ($h_1 = h_2 = 1/2$) on the flat solution curve OA.
- Unstable transient state with a rapid population change on the bifurcated path AE ($0 < h_2 < 1/2 < h_1 < 1$).
- Another stable equilibria representing a core–periphery pattern on the bifurcated path EF ($(h_1, h_2) = (1, 0)$).

Thus, the agglomeration behavior of the economy on the regular triangular lattice, despite its complexity, is analogous to that of the two-place economy, which is used as the prototype geometry in the calibration of core–periphery models of various kinds.

4.3. Robustness against parameter values

The robustness of the existence of bifurcating hexagonal distributions for Christaller's three systems is demonstrated against the change of the following two parameters that affect the agglomeration and dispersion: (1) The expenditure share μ of manufactured goods, and (2) the elasticity σ of substitution between any two varieties. Let us focus on the direct bifurcations producing $k = 3$, 4, and 7 systems. Fig. 8 shows solution curves computed for the FO model for several values of

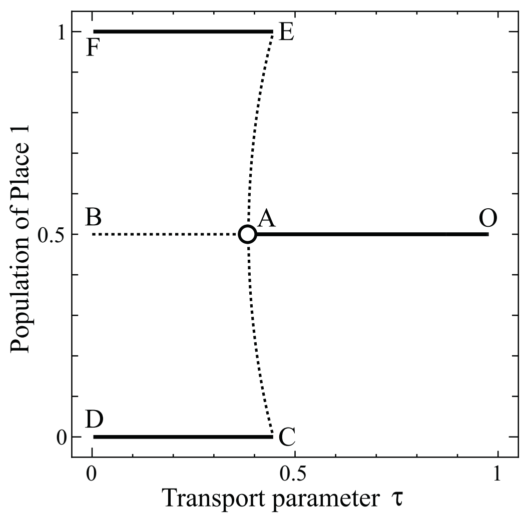

Fig. 7. Break bifurcation of the two places of the Krugman model ($\phi_{12} = 1/(1-\tau)$; solid curves: stable, dotted curves: unstable, ○: bifurcation point, $\mu = 0.4$, $\sigma = 5.0$).

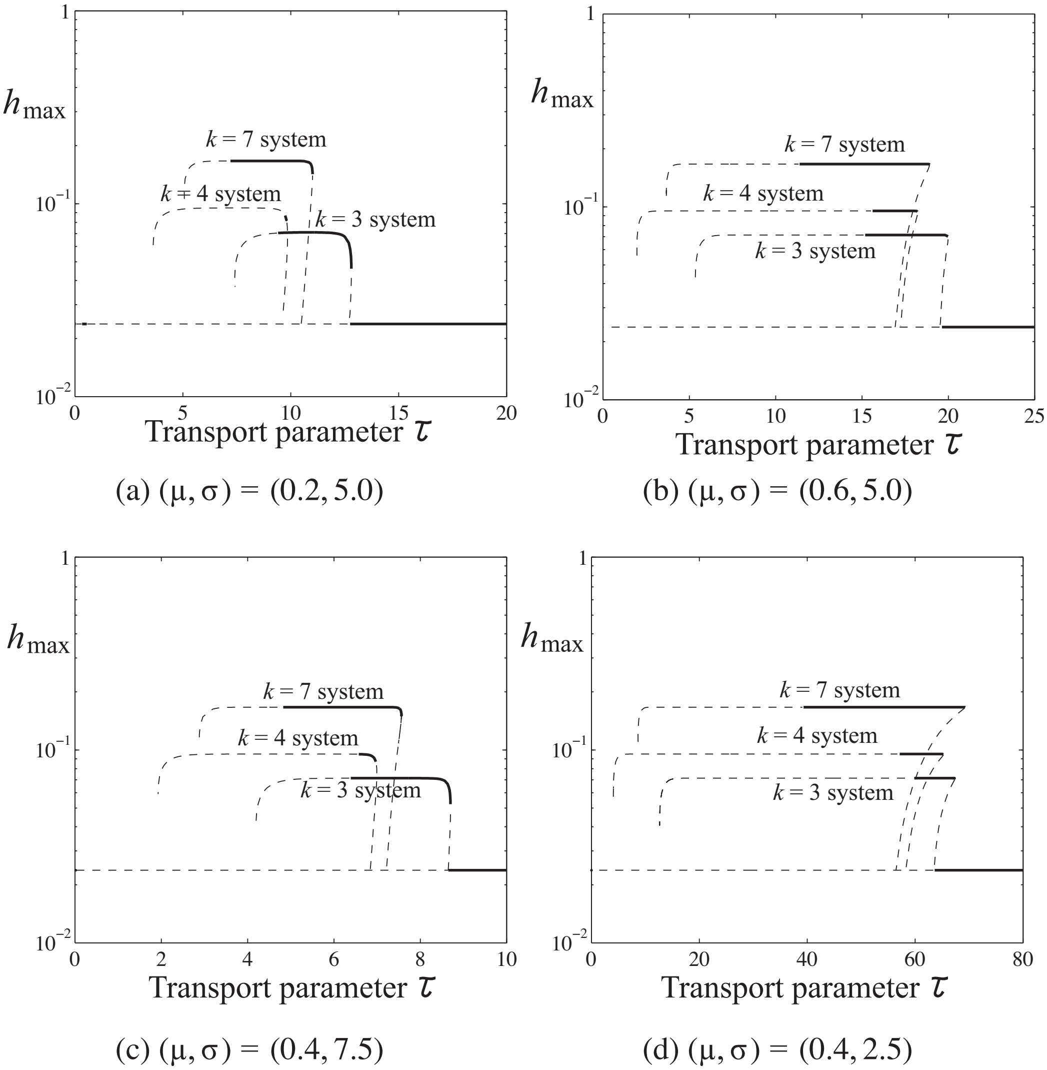

Fig. 8. Robustness of the computed results against the values of parameter μ of the utility function and constant elasticity σ of substitution between any two varieties (solid curve: stable; dashed curve: unstable). (a) $(\mu, \sigma) = (0.2, 5.0)$, (b) $(\mu, \sigma) = (0.6, 5.0)$, (c) $(\mu, \sigma) = (0.4, 7.5)$ and (d) $(\mu, \sigma) = (0.4, 2.5)$.

(μ, σ), which are to be compared with the standard case in Fig. 4 with $(\mu, \sigma) = (0.4, 5.0)$. The bifurcating curves for the $k = 3$, 4, and 7 systems exist for all values of (μ, σ) although the locations and shapes of these curves vary with parameter values. This suffices to demonstrate the robust existence of the distributions for those systems on the regular triangular lattice.

In addition, the influence of the increase of μ can be seen from Fig. 8(a) with $\mu = 0.2$ and (b) with $\mu = 0.6$ (both with $\sigma = 5.0$): The higher μ enhances the expenditure share of manufactured goods, thereby accelerating agglomeration—increasing the τ values at the bifurcation points. In contrast, the lower σ leads to greater differentiation of the variety of products, thereby accelerating agglomeration (Fig. 8(c) with $\sigma = 7.5$ and (d) with $\sigma = 2.5$ (both with $\mu = 0.4$)). Thus, the agglomeration and dispersion properties are dependent on parameter values.

5. Conclusion

For core–periphery models in new economic geography, self-organization of hexagonal population distributions for Christaller's $k = 3$, 4, and 7 systems in central place theory was investigated in this paper. The existence of those three distributions was proved and stable equilibria were actually found by computational bifurcation analysis. This confirms the prediction by Krugman (1996) of the emergence of a system of hexagonal market areas in two dimensions, thereby paving the way for cross-fertilization between central place theory and new economic geography. The emergence of the tilted hexagonal distribution for the $k = 7$ system that is directed in a different direction than the regular triangular lattice is the most phenomenal finding.

Dependence of stable equilibria on the transportation cost was investigated in view of scale economies. When the transportation cost is large, the merit of the reduction of the transportation cost for the $k=3$ system becomes predominant in comparison with the merit of scale economies for the $k=7$ system with a larger market area, and vice versa when it is small. The results of this investigation offer a theoretical foundation for *agglomeration shadow* (Arthur, 1990; Fujita et al., 1999b; Ioannides and Overman, 2004; Fujita and Mori, 2005). In the future, the agglomeration shadow should be empirically examined based on the study of two-dimensional economy.

For a *single industry*, we constructed a theoretical foundation and conducted numerical analysis based on microeconomic underpinnings, the idea of Lösch (1940), and some admittedly bold assumptions. In the future, this study should be extended to be applicable to multiple industries so as to verify Christaller's hierarchical principle, and to investigate the economic implications of the agglomeration on the regular triangular lattice in detail.

Acknowledgments

We are grateful for comments and suggestions made by Tomoya Mori and Takatoshi Tabuchi. This research was supported by Grant-in-Aid for Scientific Research (B) 19360227/21360240/ 24360202 of JSPS and the Aihara Project, the FIRST Program from JSPS, initiated by CSTP.

Appendix A. Christaller's hexagonal distributions: a review

In central place theory, the flat earth, a completely homogeneous infinite two-dimensional land surface, is introduced based on several simplifying assumptions: (i) The land surface is completely flat and homogeneous in every aspect. It is, in technical terms, an *isotropic plain*. (ii) Movement can occur in all directions with equal ease and that there is only one type of transportation. (iii) The plain is limitless or unbounded, so that complexities that tend to occur at boundaries do not need to be dealt with. (iv) The population is spread evenly over the plain.

Central place theory is developed in two steps:

(1) In the first step, for a single industry, market areas must be hexagonal in order to minimize transportation costs for a given density of central places (Lösch, 1940).
(2) In the second step, for a hierarchical structure of industries with different sizes of demand, there emerges a nested set of hexagonal market areas, which leads to the emergence of hierarchical hexagonal distributions of the population of places, such as cities, towns and villages (Christaller, 1933).

For production of bundles of goods, many levels in the hierarchy of central places appear. (Dicken and Lloyd, 1990, p. 28) stated the following:

> "Christaller's model, then, implies a fixed relationship between each level in the hierarchy. This relationship is known as a *k* value (*k* meaning a constant) and indicates that each center dominates a discrete number of lower-order centers and market areas in addition to its own."

Christaller's $k=3$, 4, and 7 systems are explained by market, traffic, and administrative principles, respectively (Christaller, 1933; Dicken and Lloyd, 1990):

For the $k=3$ system in Fig. 2(b), two neighboring first-level centers are connected by two kinked roads each of which passes a second-level center at the kink. This system is explained by Christaller's market principle of supplying the maximum number of evenly distributed consumers from a minimum number of central places.

For the $k=4$ system in Fig. 2(c), two neighboring first-level centers are connected by a straight road that passes a second-level center in agreement with Christaller's statement: "The traffic principle states that the distribution of central places is most favorable when as many important places as possible lie on one traffic route between two important towns, the route being as straightly and as cheaply as possible."

The distribution for the $k=7$ system in Fig. 2(d) agrees with Christaller's administrative principle: "The ideal of such a spatial community has the nucleus as the capital (a central place of a higher rank), around it, a wreath of satellite places of lesser importance, and toward the edge of the region a thinning population density—and even uninhabited areas."

Appendix B. Market equilibrium of core–periphery models

Two core–periphery models, the FO model and the Pf model, are introduced.

B.1. Basic assumptions

Preferences U over the M- and A-sector goods are identical across individuals. The utility of an individual in place i is

$$\text{[FO model]} \qquad U(C_i^{\mathrm{M}}, C_i^{\mathrm{A}}) = \mu \ln C_i^{\mathrm{M}} + (1-\mu) \ln C_i^{\mathrm{A}} \qquad (0 < \mu < 1), \tag{A.1a}$$

$$\text{[Pf model]} \qquad U(C_i^{\mathrm{M}}, C_i^{\mathrm{A}}) = \mu \ln C_i^{\mathrm{M}} + C_i^{\mathrm{A}} \qquad (\mu > 0), \tag{A.1b}$$

where μ is a constant parameter, C_i^{A} is the consumption of the A-sector product in place i, and C_i^{M} is the manufacturing aggregate in place i, which is defined as

$$C_i^{\mathrm{M}} \equiv \left(\sum_j \int_0^{n_j} q_{ji}(\ell)^{(\sigma-1)/\sigma} d\ell \right)^{\sigma/(\sigma-1)},$$

where $q_{ji}(\ell)$ is the consumption in place i of a variety $\ell \in [0, n_j]$ produced in place j, n_j is the continuum range of varieties produced in place j, often called the number of available varieties, and $\sigma > 1$ is the constant elasticity of substitution between any two varieties. The budget constraint is given as

$$p_i^{\mathrm{A}} C_i^{\mathrm{A}} + \sum_j \int_0^{n_j} p_{ji}(\ell) q_{ji}(\ell) d\ell = Y_i, \tag{A.2}$$

where p_i^{A} is the price of A-sector goods in place i, $p_{ji}(\ell)$ is the price of a variety ℓ in place i produced in place j and Y_i is the income of an individual in place i. The incomes (wages) of skilled workers and unskilled workers are represented, respectively, by w_i and w_i^{L}.

An individual in place i maximizes (A.1) subject to (A.2). This yields the following demand functions:

$$\text{[FO model]} \qquad C_i^{\mathrm{A}} = (1-\mu)\frac{Y_i}{p_i^{\mathrm{A}}}, \qquad C_i^{\mathrm{M}} = \mu \frac{Y_i}{\rho_i}, \qquad q_{ji}(\ell) = \mu \frac{\rho_i^{\sigma-1} Y_i}{p_{ji}(\ell)^{\sigma}}, \tag{A.3a}$$

$$\text{[Pf model]} \qquad C_i^{\mathrm{A}} = \frac{Y_i}{p_i^{\mathrm{A}}} - \mu, \qquad C_i^{\mathrm{M}} = \mu \frac{p_i^{\mathrm{A}}}{\rho_i}, \qquad q_{ji}(\ell) = \mu \frac{p_i^{\mathrm{A}} \rho_i^{\sigma-1}}{p_{ji}(\ell)^{\sigma}}, \tag{A.3b}$$

where ρ_i denotes the price index of the differentiated product in place i, which is

$$\rho_i = \left(\sum_j \int_0^{n_j} p_{ji}(\ell)^{1-\sigma} d\ell \right)^{1/(1-\sigma)}. \tag{A.4}$$

Since the total income and population in place i are $w_i h_i + w_i^{\mathrm{L}}$ and $h_i + 1$, respectively, we have the total demand $Q_{ji}(\ell)$ in place i for a variety ℓ produced in place j:

$$\text{[FO model]} \qquad Q_{ji}(\ell) = \mu \frac{\rho_i^{\sigma-1}}{p_{ji}(\ell)^{\sigma}} (w_i h_i + w_i^{\mathrm{L}}), \tag{A.5a}$$

$$\text{[Pf model]} \qquad Q_{ji}(\ell) = \mu \frac{p_i^{\mathrm{A}} \rho_i^{\sigma-1}}{p_{ji}(\ell)^{\sigma}} (h_i + 1). \tag{A.5b}$$

The A-sector is perfectly competitive and produces homogeneous goods under constant-returns-to-scale technology, which requires one unit of unskilled labor in order to produce one unit of output. For simplicity, we assume that the A-sector goods are transported between places without transportation cost and that they are chosen as the numéraire. These assumptions mean that, in equilibrium, the wage of an unskilled worker w_i^{L} is equal to the price of A-sector goods in all places (i.e., $p_i^{\mathrm{A}} = w_i^{\mathrm{L}} = 1$ for each $i = 1, \ldots, K$).

The M-sector output is produced under increasing returns to scale technology and Dixit-Stiglitz monopolistic competition. A firm incurs a fixed input requirement of α units of skilled labor and a marginal input requirement of β units of unskilled labor. That is, a linear technology in terms of unskilled labor is assumed in the profit function. Given the fixed input requirement α, the skilled labor market clearing implies $n_i = h_i/\alpha$ in equilibrium. An M-sector firm located in place i chooses $(p_{ij}(\ell) \mid j = 1, \ldots, K)$ that maximizes its profit

$$\Pi_i(\ell) = \sum_j p_{ij}(\ell) Q_{ij}(\ell) - \left(\alpha w_i + \beta x_i(\ell) \right),$$

where $x_i(\ell)$ is the total supply.

Recall that the transportation costs for M-sector goods are assumed to take the iceberg form. That is, for each unit of M-sector goods transported from place i to place $j(\neq i)$, only a fraction $1/\phi_{ij} < 1$ arrives ($\phi_{ii} = 1$). Consequently, the total supply $x_i(\ell)$ is given as

$$x_i(\ell) = \sum_j \phi_{ij} Q_{ij}(\ell). \tag{A.6}$$

Since we have a continuum of firms, each firm is negligible in the sense that its action has no impact on the market (i.e., the price indices). Therefore, the first-order condition for profit maximization yields

$$p_{ij}(\ell) = \frac{\sigma\beta}{\sigma - 1}\phi_{ij}. \tag{A.7}$$

This expression implies that the price of the M-sector products does not depend on variety ℓ, so that $Q_{ij}(\ell)$ and $x_i(\ell)$ do not depend on ℓ. Therefore, the argument ℓ is suppressed in the sequel. Substituting (A.7) into (A.4), we have the price index

$$\rho_i = \frac{\sigma\beta}{\sigma - 1}\left(\frac{1}{\alpha}\sum_j h_j d_{ji}\right)^{1/(1-\sigma)}, \tag{A.8}$$

where $d_{ji} = \phi_{ji}^{1-\sigma}$ is a spatial discounting factor between places j and i; from (A.5) and (A.8), d_{ji} is obtained as $(p_{ji}Q_{ji})/(p_{ii}Q_{ii})$, which means that d_{ji} is the ratio of total expenditure in place i for each M-sector product produced in place j to the expenditure for a domestic product.

B.2. Market equilibrium

In the short run, skilled workers are immobile between places, i.e., their spatial distribution ($\boldsymbol{h} = (h_i) \in \mathbb{R}^K$) is assumed to be given. The market equilibrium conditions consist of the M-sector goods market clearing condition and the zero-profit condition because of the free entry and exit of firms. The former condition can be written as (A.6). The latter condition requires that the operating profit of a firm be absorbed entirely by the wage bill of its skilled workers:

$$w_i(\boldsymbol{h}, \tau) = \frac{1}{\alpha}\left\{\sum_j p_{ij} Q_{ij}(\boldsymbol{h}, \tau) - \beta x_i(\boldsymbol{h}, \tau)\right\}. \tag{A.9}$$

Substituting (A.5), (A.6), (A.7), and (A.8) into (A.9), we have the market equilibrium wage:

$$[\text{FO model}] \qquad w_i(\boldsymbol{h}, \tau) = \frac{\mu}{\sigma}\sum_j \frac{d_{ij}}{\Delta_j(\boldsymbol{h}, \tau)}(w_j(\boldsymbol{h}, \tau)h_j + 1), \tag{A.10a}$$

$$[\text{Pf model}] \qquad w_i(\boldsymbol{h}, \tau) = \frac{\mu}{\sigma}\sum_j \frac{d_{ij}}{\Delta_j(\boldsymbol{h}, \tau)}(h_j + 1), \tag{A.10b}$$

where $\Delta_j(\boldsymbol{h}, \tau) \equiv \sum_k d_{kj} h_k$ denotes the market size of the M-sector in place j. Consequently, $d_{ij}/\Delta_j(\boldsymbol{h}, \tau)$ defines the market share in place j of each M-sector product produced in place i.

The indirect utility $v_i(\boldsymbol{h}, \tau)$, given the spatial distribution of the skilled workers, is obtained by substituting (A.3), (A.8), and (A.10) into (A.1) and by putting $S_i(\boldsymbol{h}, \tau) \equiv \mu(\sigma - 1)^{-1} \ln \Delta_i(\boldsymbol{h}, \tau)$:

$$[\text{FO model}] \qquad v_i(\boldsymbol{h}, \tau) = S_i(\boldsymbol{h}, \tau) + \ln[w_i(\boldsymbol{h}, \tau)], \tag{A.11a}$$

$$[\text{Pfmodel}] \qquad v_i(\boldsymbol{h}, \tau) = S_i(\boldsymbol{h}, \tau) + w_i(\boldsymbol{h}, \tau). \tag{A.11b}$$

Appendix C. Bifurcation analysis for the $n \times n$ regular triangular lattice

In this appendix, we outline a procedure of group-theoretic bifurcation analysis to arrive at bifurcation from the uniform equilibria on the regular triangular lattice, as an adaptation of Ikeda et al. (2012b).

C.1. Regular triangular lattice and hexagonal distributions

The isotropic plain in central place theory is endowed with uniformity (Appendix A). In order to express uniformity, let us introduce a finite regular triangular lattice in the xy-plane comprising uniformly distributed $n \times n$ places with periodic boundaries (Fig. 1(a) for $n = 4$).

A place is allocated at each node of the regular triangular lattice, expressed by

$$\boldsymbol{p} = n_1\boldsymbol{\ell}_1 + n_2\boldsymbol{\ell}_2, \quad n_1, n_2 = 1, \ldots, n,$$

where $\ell_1 = (d, 0)^\top$ and $\ell_2 = (-d/2, d\sqrt{3}/2)^\top$ are oblique basis vectors. Two neighboring places are connected by a straight road with nominal length d, as shown in Fig. 1(a) for a 4×4 regular triangular lattice.

Equilibria of various kinds branch from the uniform (flat earth) equilibria on the regular triangular lattice. If an equilibrium has two-dimensional periodicity, then we can set a pair of independent vectors $(\boldsymbol{t}_1, \boldsymbol{t}_2)$ such that the equilibrium remains invariant under the translations along these vectors.

Among a plethora of patterns of equilibria on this lattice, we focus on hexagonal ones, which are given by

$$\boldsymbol{t}_1 = \alpha\boldsymbol{\ell}_1 + \beta\boldsymbol{\ell}_2, \quad \boldsymbol{t}_2 = -\beta\boldsymbol{\ell}_1 + (\alpha - \beta)\boldsymbol{\ell}_2, \tag{A.12}$$

where α and β are positive integers and the angle between $\boldsymbol{t}_1$ and $\boldsymbol{t}_2$ is $2\pi/3$. The spatial period is given by $L = \| \boldsymbol{t}_1 \| = \| \boldsymbol{t}_2 \|$, and we have

$$L/d = \sqrt{(\alpha - \beta/2)^2 + (\beta\sqrt{3}/2)^2} = \sqrt{\alpha^2 - \alpha\beta + \beta^2}. \tag{A.13}$$

We introduce a positive integer

$$k = \alpha^2 - \alpha\beta + \beta^2, \tag{A.14}$$

which can take some specific values, such as 1, 3, 4, 7, ... The values of (α, β) for $k = 1, 3, 4,$ and 7 are given uniquely as

$$(\alpha, \beta) = \begin{cases} (1, 0): & \text{uniform distribution} \, (k = 1), \\ (2, 1): & k = 3 \, \text{system}, \\ (2, 0): & k = 4 \, \text{system}, \\ (3, 1): & k = 7 \, \text{system}. \end{cases}$$

Then (A.13) with (A.14) gives Lösch's formula (5). The spatial period vectors are given by

$$(\boldsymbol{t}_1, \boldsymbol{t}_2) = \begin{cases} (\boldsymbol{\ell}_1, \boldsymbol{\ell}_2): & \text{uniform distribution} \, (k = 1), \\ (2\boldsymbol{\ell}_1 + \boldsymbol{\ell}_2, -\boldsymbol{\ell}_1 + \boldsymbol{\ell}_2): & k = 3 \, \text{system}, \\ (2\boldsymbol{\ell}_1, 2\boldsymbol{\ell}_2): & k = 4 \, \text{system}, \\ (3\boldsymbol{\ell}_1 + \boldsymbol{\ell}_2, -\boldsymbol{\ell}_1 + 2\boldsymbol{\ell}_2): & k = 7 \, \text{system}. \end{cases}$$

The population distribution $\boldsymbol{h}$ for Christaller's $k = 3, 4,$ and 7 systems can be given as

$$\boldsymbol{h} = \begin{cases} (a, b, b; b, b, a; b, a, b)^\top, & \text{for } k = 3 \, \text{system} \, (n = 3), \\ (a, b; b, b)^\top, & \text{for } k = 4 \, \text{system} \, (n = 2), \\ (a, b, b, b, b, b, b; b, b, b, a, b, b, b; b, b, b, b, b, b, a; b, b, a, b, b, b, & \\ b; b, b, b, b, b, a, b; b, a, b, b, b, b, b; b, b, b, b, a, b, b)^\top, & \text{for } k = 7 \, \text{system} \, (n = 7), \end{cases} \tag{A.15}$$

where a and b are nonnegative.

C.2. Symmetries of hexagonal distributions

The regular triangular lattice is invariant with respect to the following four transformations

$$\begin{cases} r: & \text{counterclockwise rotation about the origin at an angle of } \pi/3, \\ s: & \text{reflection } y \mapsto -y, \\ p_1: & \text{the } \boldsymbol{\ell}_1\text{-axis (i.e., the } x\text{-axis)}, \\ p_2: & \text{periodic translation along the } \boldsymbol{\ell}_2\text{-axis}, \end{cases} \tag{A.16}$$

and its symmetry is characterized by the group generated by those four transformations:

$$G = \langle r, s, p_1, p_2 \rangle. \tag{A.17}$$

Among many subgroups[16] of $G = \langle r, s, p_1, p_2\rangle$, which express partial symmetries of the regular triangular lattice, we are interested in those subgroups expressing hexagons for Christaller's $k = 3$, 4, and 7 systems:

$$G' = \begin{cases} \langle r, s, p_1^2 p_2, p_1^{-1} p_2\rangle & \text{for } k = 3 \text{ system,} \\ \langle r, s, p_1^2, p_2^2\rangle & \text{for } k = 4 \text{ system,} \\ \langle r, p_1^3 p_2, p_1^{-1} p_2^2\rangle & \text{for } k = 7 \text{ system.} \end{cases} \tag{A.18}$$

From the translational symmetry, we can derive a compatibility condition for the size n of the regular triangular lattice for a specified k value:

- For $k = 3$ with $(\alpha, \beta) = (2, 1)$, we have $(p_1^2 p_2) \times (p_1^{-1} p_2)^{-1} = p_1^3$, which represents a translation in the direction of the ℓ_1-axis at a length of $3d$; accordingly, n must be a multiple of 3.
- For $k = 4$ with $(\alpha, \beta) = (2, 0)$, the symmetry of p_1^2 and p_2^2 implies that n is a multiple of 2.
- For $k = 7$ with $(\alpha, \beta) = (3, 1)$, we have $(p_1^3 p_2)^2 \times (p_1^{-1} p_2^2)^{-1} = p_1^7$, from which follows that n is a multiple of 7.

C.3. Symmetry of bifurcating equilibria

A procedure to determine the symmetry of bifurcating equilibria is explained.

C.3.1. Outline

The equilibria (solutions) of the spatial equilibrium condition (2) are divided into ordinary points and critical points, according to whether its *Jacobian matrix* $J = (J_{ij}) = (\partial F_i/\partial h_j)$, which is a $K \times K$ matrix, is nonsingular or singular. A critical point is further classified into a bifurcation point and a limit (local maximum or minimum) point of τ.

The symmetry-breaking bifurcation has several properties:

- Property 1: The symmetry of the equilibrium points is preserved until branching into a bifurcated curve.
- Property 2: The symmetry of equilibria on a bifurcated path is labeled by a subgroup, say G_1, of the group G.
- Property 3: In association with repeated bifurcations, one can find a hierarchy of subgroups $G \longrightarrow G_1 \longrightarrow G_2 \longrightarrow \cdots$ that characterizes the hierarchical change of symmetries. Here $\longrightarrow$ denotes a bifurcation.

C.3.2. Proof of equivariance of core–periphery models

The equivariance (8) (Lemma 1)

$$T(g)\boldsymbol{F}(\boldsymbol{h}, \tau) = \boldsymbol{F}(T(g)\boldsymbol{h}, \tau), \qquad g \in G \tag{A.19}$$

is proved for the group $G = \langle r, s, p_1, p_2\rangle$ in (A.17) and

$$\boldsymbol{F}(\boldsymbol{h}, \tau) = H\boldsymbol{P}(\boldsymbol{v}(\boldsymbol{h}, \tau)) - \boldsymbol{h} \tag{A.20}$$

in (3) for core–periphery models.

As a preliminary, we investigate the symmetry condition of the functions $\boldsymbol{v}(\boldsymbol{h}, \tau)$ and $\boldsymbol{P}(\boldsymbol{v})$ in these core–periphery models on the $n \times n$ regular triangular lattice. On this lattice, each element g of G acts as a permutation among place numbers $(1, \ldots, K)$ with $K = n^2$ places. Let $T(g)$ be a permutation matrix, expressing the permutation

$$i \mapsto i^* \tag{A.21}$$

of place numbers $i = 1, \ldots, K$ caused by $g \in G$. The action in (A.21) entails

$$h_i \mapsto h_{i^*}, \quad v_i \mapsto v_{i^*}, \quad P_i \mapsto P_{i^*}, \tag{A.22}$$

which are expressed, respectively, by the same permutation matrix $T(g)$ as

$$T(g)\boldsymbol{h}, \quad T(g)\boldsymbol{v}, \quad T(g)\boldsymbol{P}. \tag{A.23}$$

The symmetry conditions for the indirect utility function vector $\boldsymbol{v}(\boldsymbol{h}, \tau)$ and the choice function vector $\boldsymbol{P}$ are given in the following lemma.

Lemma 2. *The indirect utility function vector satisfies the symmetry condition*

$$T(g)\boldsymbol{v}(\boldsymbol{h}, \tau) = \boldsymbol{v}(T(g)\boldsymbol{h}, \tau), \qquad g \in G. \tag{A.24}$$

[16] A subgroup of a group G is a subset of G that forms a group with respect to the operation in G and expresses the partial symmetry of the one represented by G.

The choice function vector satisfies the symmetry condition

$$T(g)\boldsymbol{P}(v) = \boldsymbol{P}(T(g)v), \qquad g \in G. \tag{A.25}$$

Proof. The symmetry condition (A.24) is proved as follows. The action of g on the vector $\boldsymbol{v}(\boldsymbol{h}, \tau)$ is expressed as

$$g : (v_1(\boldsymbol{h}, \tau), \ldots, \overset{i}{v_i(\boldsymbol{h}, \tau)}, \ldots, v_K(\boldsymbol{h}, \tau)) \mapsto (\ldots, \overset{i^*}{v_i(T(g)\boldsymbol{h}, \tau)}, \ldots),$$

in which the components of $\boldsymbol{h}$ and those of $\boldsymbol{v}$ are simultaneously permuted by $g : i \mapsto i^*$. This means that the indirect utility at the i^*th place, which is $v_{i^*}(\boldsymbol{h}, \tau)$ before the action of g, is expressed as $v_i(T(g)\boldsymbol{h}, \tau)$ after this action. Since the utility before the action and that after the action must be identical, we have

$$v_{i^*}(\boldsymbol{h}, \tau) = v_i(T(g)\boldsymbol{h}, \tau), \quad g \in G, \tag{A.26}$$

which shows (A.24). The condition (A.25) can be shown by the explicit form (4) of the function $\boldsymbol{P}(\boldsymbol{v})$.

From (A.24) and (A.25) in Lemma 2, we have

$$T(g)\boldsymbol{P}(\boldsymbol{v}(\boldsymbol{h}, \tau)) = \boldsymbol{P}(T(g)\boldsymbol{v}(\boldsymbol{h}, \tau)) = \boldsymbol{P}(\boldsymbol{v}(T(g)\boldsymbol{h}, \tau)), \quad g \in G.$$

Therefore, we have

$$T(g)\boldsymbol{F}(\boldsymbol{h}, \tau) = H\boldsymbol{P}(\boldsymbol{v}(T(g)\boldsymbol{h}, \tau)) - T(g)\boldsymbol{h} = \boldsymbol{F}(T(g)\boldsymbol{h}, \tau), \quad g \in G.$$

This proves the equivariance (A.19).

C.3.3. Method of group-theoretic bifurcation analysis

The group-theoretic bifurcation analysis at a critical point, say $(\boldsymbol{h}_c, \tau_c)$, of multiplicity $M(\geq 1)$ proceeds as follows. The full system of equations (2), $\boldsymbol{F}(\boldsymbol{h}, \tau) = \boldsymbol{0}$ in $\boldsymbol{h}$, can be reduced,[17] in a neighborhood of $(\boldsymbol{h}_c, \tau_c)$, to a system of M equations

$$\tilde{\boldsymbol{F}}(\boldsymbol{w}, \tilde{\tau}) = \boldsymbol{0} \tag{A.27}$$

in an M-dimensional vector $\boldsymbol{w}$, where $\tilde{\boldsymbol{F}}$ is an M-dimensional function vector and $\tilde{\tau} = \tau - \tau_c$ denotes the increment of τ. The reduced system (A.27) is called the bifurcation equation. In this reduction process, the equivariance of the full system, which is formulated in (A.19), is inherited by the reduced system (A.27) in the following form:

$$\tilde{T}(g)\tilde{\boldsymbol{F}}(\boldsymbol{w}, \tilde{\tau}) = \tilde{\boldsymbol{F}}(\tilde{T}(g)\boldsymbol{w}, \tilde{\tau}), \qquad g \in G, \tag{A.28}$$

where $\tilde{T}$ is the subrepresentation of T in the M-dimensional kernel space of the Jacobian matrix at the critical point $(\boldsymbol{h}_c, \tau_c)$. It is this inheritance of symmetry that restricts $\tilde{\boldsymbol{F}}$ to be a special form.

The reduced equation $\tilde{\boldsymbol{F}} = \boldsymbol{0}$ in (A.27) with such a special form is to be solved for $\boldsymbol{w}$ as $\boldsymbol{w} = \boldsymbol{w}(\tilde{\tau})$. Since $(\boldsymbol{w}, \tilde{\tau}) = (\boldsymbol{0}, 0)$ is a critical point of (A.27), there can be many equilibria $\boldsymbol{w} = \boldsymbol{w}(\tilde{\tau})$ with $\boldsymbol{w}(0) = \boldsymbol{0}$, which give rise to bifurcation. Each $\boldsymbol{w}$ uniquely determines an equilibrium $\boldsymbol{h}$ of the full system (2). The symmetry of $\boldsymbol{h}$ can be computed in terms of the symmetry of the corresponding $\boldsymbol{w}$ and is expressed by a subgroup of the group G.

The symmetry of $\boldsymbol{h}$ is represented by a subgroup of G defined by

$$\Sigma(\boldsymbol{h}; G, T) = \{g \in G \mid T(g)\boldsymbol{h} = \boldsymbol{h}\}, \tag{A.29}$$

called the isotropy subgroup of $\boldsymbol{h}$. The isotropy subgroup $\Sigma(\boldsymbol{h})$ can be computed in terms of the symmetry of the corresponding $\boldsymbol{w}$ as

$$\Sigma(\boldsymbol{h}; G, T) = \Sigma(\boldsymbol{w}; G, \tilde{T}), \tag{A.30}$$

where

$$\Sigma(\boldsymbol{w}; G, \tilde{T}) = \{g \in G \mid \tilde{T}(g)\boldsymbol{w} = \boldsymbol{w}\}. \tag{A.31}$$

The relation (A.30) enables us to determine the symmetry of bifurcating solutions $\boldsymbol{h}$ through the analysis of bifurcation equations in $\boldsymbol{w}$.

C.4. Simple example

The method described in Section C.3 is illustrated here for the two-place economy (Fujita et al., 1999b). Consider Place 1 and Place 2 with a population of h_1 and h_2 $(K = 2)$, respectively, that satisfy the conservation law $h_1 + h_2 = 1$ of population.

[17] This reduction is the standard procedure called the *Liapunov–Schmidt reduction with symmetry* (Sattinger, 1979; Golubitsky et al., 1988).

These two identical places are invariant with respect to the reflection s that permutes Place 1 and Place 2, as well as the identity element e that leaves everything unchanged ($s^2 = e$). That is, the symmetry of the two-place economy is described by a group of reflection $G = \{e, s\}$. The action of this group is represented by matrices

$$T(e) = \begin{bmatrix} 1 & 0 \\ 0 & 1 \end{bmatrix}, \qquad T(s) = \begin{bmatrix} 0 & 1 \\ 1 & 0 \end{bmatrix}.$$

The equivariance condition (cf., (A.19)) reduces to

$$\begin{bmatrix} 0 & 1 \\ 1 & 0 \end{bmatrix} \begin{bmatrix} F_1(h_1, h_2, \tau) \\ F_2(h_1, h_2, \tau) \end{bmatrix} = \boldsymbol{F}(\begin{bmatrix} 0 & 1 \\ 1 & 0 \end{bmatrix} \begin{bmatrix} h_1 \\ h_2 \end{bmatrix}, \tau),$$

which is equivalent to

$$\begin{cases} F_2(h_1, h_2, \tau) = F_1(h_2, h_1, \tau), \\ F_1(h_1, h_2, \tau) = F_2(h_2, h_1, \tau). \end{cases} \tag{A.32}$$

The pre-bifurcation flat earth (uniform) equilibria take the form of $(h_1, h_2, \tau) = (1/2, 1/2, \tau)$. On these equilibria, a critical point $(\boldsymbol{h}_c, \tau_c) = (1/2, 1/2, \tau_c)$ might be encountered at $\tau = \tau_c$ for some τ_c. The variables $w = h_1 - h_2$ and $\tilde{\tau} = \tau - \tau_c$ are defined, and then, from $\boldsymbol{F} = (F_1, F_2)^\top = \boldsymbol{0}$ with the symmetry condition (A.32), the bifurcation equation (with $M = 1$) can be obtained (Ikeda and Murota, 2010, §7.2):

$$\begin{aligned} \tilde{F}(w, \tilde{\tau}) &= F_1(\frac{(1+w)}{2}, \frac{(1-w)}{2}, \tilde{\tau}) - F_2(\frac{(1+w)}{2}, \frac{(1-w)}{2}, \tilde{\tau}) \\ &= w[A\tilde{\tau} + Bw^2 + (\text{higher order terms})] = 0 \end{aligned} \tag{A.33}$$

(for some constants A and B). The equivariance condition (A.28) for the bifurcation equation is indeed satisfied with $\tilde{T}$ given by

$$\tilde{T}(e) = 1, \qquad \tilde{T}(s) = -1.$$

The bifurcation equation (A.33) has two kinds of equilibria:

$$\begin{cases} w = 0, & \text{flat earth equilibria } (h_1 = h_2), \\ \tilde{\tau} = -\dfrac{B}{A}w^2 + (\text{higher order terms}), & \text{bifurcatedequilibria } (h_1 \neq h_2). \end{cases}$$

The pre-bifurcation flat earth equilibria $w = 0$ ($h_1 = h_2 = 1/2$) have the reflection symmetry labeled $G = \{e, s\}$, while the bifurcating equilibria do not have any symmetry (labeled $G' = \{e\}$).

C.5. Analysis by equivariant branching lemma

The emergence of Christaller's hexagons can be proved by applying the equivariant branching lemma to the bifurcation equation $\tilde{\boldsymbol{F}}(\boldsymbol{w}, \tilde{\tau})$ in (A.27); see, e.g., Golubitsky et al. (1988) for this lemma and related fundamental facts. It is known that the bifurcation equation is associated with an irreducible representation of G and that the isotropy subgroup $\Sigma(\boldsymbol{h})$ in (A.29) expressing the symmetry of a bifurcated solution $\boldsymbol{h}$ is identical with the isotropy subgroup $\Sigma(\boldsymbol{w})$ in (A.31) of the corresponding solution $\boldsymbol{w}$ for the bifurcation equation, i.e., $\Sigma(\boldsymbol{h}) = \Sigma(\boldsymbol{w})$, as shown in (A.30). A subgroup Σ is said to be an isotropy subgroup if $\Sigma = \Sigma(\boldsymbol{h})$ for some $\boldsymbol{h}$.

The analysis based on the equivariant branching lemma has the following steps:

1. Specify an isotropy subgroup Σ of G for the symmetry of a possible bifurcating solution as well as an irreducible representation $\tilde{T}$ of G that can possibly be associated with the bifurcation point.
2. Obtain a fixed-point subspace $\mathrm{Fix}(\Sigma)$ for the isotropy subgroup Σ with respect to the irreducible representation $\tilde{T}$, where

$$\mathrm{Fix}(\Sigma) = \{\boldsymbol{w} \in \mathbb{R}^M \mid \tilde{T}(g)\boldsymbol{w} = \boldsymbol{w} \text{ for all } g \in \Sigma\}. \tag{A.34}$$

3. Calculate the dimension $\dim \mathrm{Fix}(\Sigma)$ of this subspace.
4. If $\dim \mathrm{Fix}(\Sigma) = 1$, a bifurcating solution with symmetry Σ is guaranteed to exist generically by the equivariant branching lemma.

In the present analysis, the above procedure is employed with $\Sigma = G'$ for each G' in (A.18) and for each irreducible representation $\tilde{T}$ of G; note that each G', representing the symmetry of a Christaller's hexagon, is an isotropy subgroup. The dimension of $\tilde{T}$, which is equal (generically) to the multiplicity M of the critical point, is either 1, 2, 3, 4, 6, or 12.

The main message is that such bifurcated equilibria do exist, and therefore these systems can be understood within the framework of group-theoretic bifurcation theory. The hexagonal distributions for Christaller's $k = 3$, 4, and 7 systems emerge from bifurcation points of multiplicity $M = 2$, 3, 12, respectively, but not of $M = 1$, 4, 6.

C.5.1. k = 3 system

When n is a multiple of 3, hexagonal patterns for Christaller's $k = 3$ system are predicted to branch from a bifurcation point that is associated with the irreducible representation of $G = \langle r, s, p_1, p_2 \rangle$ given by

$$\tilde{T}(r) = \begin{bmatrix} 1 & 0 \\ 0 & -1 \end{bmatrix}, \tilde{T}(s) = \begin{bmatrix} 1 & 0 \\ 0 & 1 \end{bmatrix}, \tilde{T}(p_1) = \tilde{T}(p_2) = \begin{bmatrix} \cos(2\pi/3) & -\sin(2\pi/3) \\ \sin(2\pi/3) & \cos(2\pi/3) \end{bmatrix}. \tag{A.35}$$

Since this is two-dimensional, the multiplicity of the bifurcation point is $M = 2$.

In the search for a bifurcating hexagonal distribution, let us follow the steps of the aforementioned analysis procedure as follows:

1. Specify

$$\Sigma = \langle r, s, p_1^2 p_2, p_1^{-1} p_2 \rangle, \tag{A.36}$$

which is an isotropy subgroup describing the symmetry of the hexagon for Christaller's $k = 3$ system in Fig. 2(b).

2. The fixed-point subspace $\mathrm{Fix}(\Sigma)$ in (A.34) with respect to $\tilde{T}$ in (A.35) is given as

$$\mathrm{Fix}(\Sigma) = \{\boldsymbol{w} \in \mathbb{R}^2 \mid \boldsymbol{w} = c(1, 0)^\top, \ c \in \mathbb{R}\}$$

because

$$\tilde{T}(r)\boldsymbol{w} = \boldsymbol{w}$$

holds if and only if $\boldsymbol{w} = c(1, 0)^\top$ for some $c \in \mathbb{R}$, and

$$\tilde{T}(s)\boldsymbol{w} = \boldsymbol{w}, \quad \tilde{T}(p_1^2 p_2)\boldsymbol{w} = \boldsymbol{w}, \quad \tilde{T}(p_1^{-1} p_2)\boldsymbol{w} = \boldsymbol{w}$$

are satisfied by all $\boldsymbol{w}$, where we used the relations

$$\tilde{T}(p_1^2 p_2) = \tilde{T}(p_1)^2 \tilde{T}(p_2) = \begin{bmatrix} 1 & 0 \\ 0 & 1 \end{bmatrix}, \quad \tilde{T}(p_1^{-1} p_2) = \tilde{T}(p_1)^{-1} \tilde{T}(p_2) = \begin{bmatrix} 1 & 0 \\ 0 & 1 \end{bmatrix}.$$

3. $\dim \mathrm{Fix}(\Sigma) = 1$.
4. Since $\dim \mathrm{Fix}(\Sigma) = 1$, a bifurcating solution with symmetry Σ in (A.36) exists by the equivariant branching lemma.

C.5.2. k = 4 system

When n is a multiple of 2, hexagonal patterns for the $k = 4$ system are predicted to branch from a bifurcation point that is associated with the three-dimensional irreducible representation of $G = \langle r, s, p_1, p_2 \rangle$ given by

$$\tilde{T}(r) = \begin{bmatrix} 0 & 0 & 1 \\ 1 & 0 & 0 \\ 0 & 1 & 0 \end{bmatrix}, \qquad \tilde{T}(s) = \begin{bmatrix} 0 & 0 & 1 \\ 0 & 1 & 0 \\ 1 & 0 & 0 \end{bmatrix}; \tag{A.37}$$

$$\tilde{T}(p_1) = \begin{bmatrix} -1 & 0 & 0 \\ 0 & 1 & 0 \\ 0 & 0 & -1 \end{bmatrix}, \qquad \tilde{T}(p_2) = \begin{bmatrix} 1 & 0 & 0 \\ 0 & -1 & 0 \\ 0 & 0 & -1 \end{bmatrix}. \tag{A.38}$$

The multiplicity of the bifurcation point is $M = 3$.

The general procedure is applied to

$$\Sigma = \langle r, s, p_1^2, p_2^2 \rangle, \tag{A.39}$$

which is an isotropy subgroup expressing the symmetry of the hexagon for Christaller's $k=4$ system in Fig. 2(c). The fixed-point subspace Fix(Σ) in (A.34) with respect to $\tilde{T}$ in (A.37) and (A.38) is a one-dimensional subspace of $\mathbb{R}^3$ spanned by $(1, 1, 1)^\top$. Then, by the equivariant branching lemma, a bifurcating path with the symmetry of (A.39) exists.

C.5.3. k = 7 system

When n is a multiple of 7, hexagonal patterns for the $k=7$ system are predicted to branch from a bifurcation point associated with a 12-dimensional irreducible representation. The multiplicity of the bifurcation point is $M=12$. It can be shown, according to the aforementioned analysis procedure, that there exists a bifurcating solution with the symmetry

$$\langle r, p_1^3 p_2, p_1^{-1} p_2^2 \rangle \tag{A.40}$$

associated (see (A.18)) with the tilted hexagon for the $k=7$ system in Fig. 2(d). See Ikeda et al. (2012b) for details.

References

Akamatsu, T., Takayama, Y., Ikeda, K., 2012. Spatial discounting, Fourier, and racetrack economy: a recipe for the analysis of spatial agglomeration models. Journal of Economic Dynamics and Control 36 (11), 1729–1759.

Anderson, S.P., de Palma, A., Thisse, J.-F., 1992. Discrete Choice Theory of Product Differentiation. MIT Press, Cambridge, MA.

Arthur, W.B., 1990. 'Silicon Valley' locational clusters: when do increasing returns imply monopoly? Mathematical Social Sciences 19 (3), 235–251.

Barker, D., 2012. Slime mold cities. Environment and Planning B: Planning and Design 39, 262–286.

Behrens, K., Thisse, J.-F., 2007. Regional economics: a new economic geography perspective. Regional Science and Urban Economics 37 (4), 457–465.

Bosker, M., Brakman, S., Garretsen, H., Schramm, M., 2010. Adding geography to the new economic geography: bridging the gap between theory and empirics. Journal of Economic Geography 10, 793–823.

Christaller, W., 1933. Die Zentralen Orte in Süddeutschland. Gustav Fischer, Jena (English translation: Central Places in Southern Germany, Prentice Hall, Englewood Cliffs, 1966).

Clarke, M., Wilson, A.G., 1985. The dynamics of urban spatial structure: the progress of a research programme. Transactions of the Institute of British Geographers, New Series 10 (4), 427–451.

Dicken, P., Lloyd, P.E., 1990. Location in Space: Theoretical Perspectives in Economic Geography, 3rd ed. Harper Collins, New York.

Dixit, A., Stiglitz, J., 1977. Monopolistic competition and optimum product diversity. American Economic Review 67, 297–308.

Eaton, B.C., Lipsey, R.G., 1975. The principle of minimum differentiation reconsidered: some new developments in the theory of spatial competition. The Review of Economic Studies 42 (1), 27–49.

Eaton, B.C., Lipsey, R.G., 1982. An economic theory of central places. Economic Journal 92 (365), 56–72.

Flam, H., Helpman, E., 1987. Industrial policy under monopolistic competition. Journal of International Economics 22, 79–102.

Forslid, R., Ottaviano, G.I.P., 2003. An analytically solvable core–periphery model. Journal of Economic Geography 3, 229–340.

Fudenberg, D., Levine, D.K., 1998. The Theory of Learning in Games. MIT Press, Cambridge, MA.

Fujita, M., Krugman, P., Mori, T., 1999a. On the evolution of hierarchical urban systems. European Economic Review 43 (2), 209–251.

Fujita, M., Krugman, P., Venables, A.J., 1999b. The Spatial Economy: Cities, Regions, and International Trade. MIT Press, Cambridge, MA.

Fujita, M., Mori, T., 2005. Frontiers of the New Economic Geography. Papers in Regional Science 84 (3), 377–405.

Golubitsky, M., Stewart, I., 2002. The Symmetry Perspective. Birkhäuser Verlag, Basel.

Golubitsky, M., Stewart, I., Schaeffer, D.G., 1988. Singularities and Groups in Bifurcation Theory, Vol. 2. Springer-Verlag, New York.

Hofbauer, J., Sandholm, W.H., 2007. Evolution in games with randomly disturbed payoffs. Journal of Economic Theory 132, 47–69.

Ikeda, K., Akamatsu, T., Kono, T., 2012a. Spatial period-doubling agglomeration of a core–periphery model with a system of cities. Journal of Economic Dynamics and Control 36, 754–778.

Ikeda, K., Murota, K., 2010. Imperfect Bifurcation in Structures and Materials, 2nd ed. Springer-Verlag, New York.

Ikeda, K., Murota, K., Akamatsu, T., 2012b. Self-organization of Lösch's hexagons in economic agglomeration for core-periphery models. International Journal of Bifurcation and Chaos 22 (8), 1230026-1–1230026-29.

Ioannides, Y.M., Overman, H.G., 2004. Spatial evolution of the US urban system. Journal of Economic Geography 4 (2), 131–156.

Koschmieder, E.L., 1974. Benard convection. Advances in Chemical Physic 26, 177–188.

Krugman, P., 1991. Increasing returns and economic geography. Journal of Political Economy 99, 483–499.

Krugman, P., 1993. On the number and location of cities. European Economic Review 37, 293–298.

Krugman, P., 1996. The Self-Organizing Economy. Blackwell, Oxford.

Lösch, A., 1940. Die räumliche Ordnung der Wirtschaft. Gustav Fischer, Jena (English translation: The Economics of Location, Yale University, New Haven, 1954).

Martin, P.J., Rogers, C.A., 1995. Trade effects of regional aid. In: Baldwin, R., Haaparanta, P., Kiander, J. (Eds.), Expanding Membership of the European Union. Cambridge University Press, Cambridge, UK, pp. 166–188.

McFadden, D., 1974. Conditional Logit Analysis of Qualitative Choice Behavior. In: Zarembka, P. (Ed.), Frontiers in Econometrics. Academic Press, New York, pp. 105–142.

Munz, M., Weidlich, W., 1990. Settlement formation, Part II: Numerical simulation. The Annals of Regional Science 24, 177–196.

Murata, Y., 2003. Product diversity, taste heterogeneity, and geographic distribution of economic activities: market vs. non-market interactions. Journal of Urban Economics 53 (1), 126–144.

Neary, J.P., 2001. Of hype and hyperbolas: introducing the new economic geography. Journal of Economic Literature 39, 536–561.

Pflüger, M., 2004. A simple, analytically solvable, chamberlinian agglomeration model. Regional Science and Urban Economics 34, 565–573.

Picard, P.M., Tabuchi, T., 2010. Self-organized agglomerations and transport costs. Economic Theory 42, 565–589.

Sandholm, W.H., 2010. Population Games and Evolutionary Dynamics. MIT Press, Cambridge, MA.

Sanglier, M., Allen, P., 1989. Evolutionary models of urban systems: an application to the Belgian provinces. Environment and Planning A 21, 477–498.

Sattinger, D.H., 1979. Group Theoretic Methods in Bifurcation Theory. Springer-Verlag, Berlin.

Stelder, D., 2005. Where do cities form? A geographical agglomeration model for Europe. Journal of Regional Science 45, 657–679.

Tabuchi, T., Thisse, J.-F., 2002. Taste heterogeneity, labor mobility and economic geography. Journal of Development Economics 69, 155–177.

Tabuchi, T., Thisse, J.-F., 2011. A new economic geography model of central places. Journal of Urban Economics 69, 240–252.